Prediction of Molecular Properties Including Symmetry from Quantum-Based Molecular Structural Formulas, VIF

Joseph D. Alia,* Bess Vlaisavljevich, Matthew Abbot, Hallie Warneke, and Tyson Mastin

University of Minnesota, Morris, Division of Science and Math, 600 East Fourth Street, Morris, Minnesota 56267

Received: December 21, 2007; Revised Manuscript Received: May 22, 2008

Structurally covariant valency interaction formulas, VIF, gain chemical significance by comparison with resonance structures and natural bond orbital, NBO, bonding schemes and at the same time allow for additional prediction such as symmetry of ring systems and destabilization of electron pairs with respect to reference energy of $-1/2\,E_h$. Comparisons are based on three chemical interpretations of Sinanoğlu's theory of structural covariance: (1) sets of structurally covariant quantum structural formulas, VIF, are interpreted as the same quantum operator represented in linearly related basis frames; (2) structurally covariant VIF pictures are interpreted as sets of molecular species with similar energy; and (3) the same VIF picture can be interpreted as different quantum operators, one-electron density or Hamiltonian; for example. According to these three interpretations, bond pair, lone pair, and free radical electrons understood in terms of a localized orbital representation are recognized as having energies above, below, or equal to a predetermined reference, frequently $-1/2\,E_h$. The probable position of electron pairs and radical electrons is predicted. The selectivity of concerted ring closures in allyl anion and cation is described. Symmetries of conjugated ring systems are predicted according to their numbers of π-electrons and spin-multiplicity. The π-distortivity of benzene is predicted. The 3c/2e$^-$ H-bridging bonds in diborane are derived in a natural way according to the notion that the bridging bonds will have delocalizing interactions between them consistent with results of the NBO method. Key chemical bonding motifs are described using VIF. These include 2c/1e$^-$, 2c/2e$^-$, 2c/3e$^-$, 3c/2e$^-$, 3c/3e$^-$, 3c/4e$^-$, 4n antiaromatic, and 4n+2 aromatic bonding systems. Some common organic functional groups are represented as VIF pictures and because these pictures can be interpreted simultaneously as one-electron density and Hamiltonian operators, the valence shell electron pair repulsion method is applied toward understanding the energies of valence NBOs with respect to the reference energy of $-1/2E_h$.

I. Introduction

The application of quantum mechanical reasoning to molecular structural formulas began soon after the inception of quantum mechanics in the mid 1920s.[1] The idea of mesomerism,[2] later to be known as resonance, is a staple of qualitative reasoning in chemistry. Notions of hybridization and resonance rationalize bond lengths and angles in a wide variety of organic molecules. In addition, the notion of resonance stabilization has been helpful for summarizing a great deal of chemical reactivity. Other properties like the high symmetry of aromatic rings and the simultaneous distortion of antiaromatic rings are more easily understood through the use of qualitative molecular orbital ideas. One can just as easily draw resonance structures for the benzene molecule as for cyclobutadiene but for benzene the carbon-carbon bond lengths are the same and in singlet cyclobutadiene there are distinct single and double bonds. This difference can be understood as a Jahn–Teller distortion[3] and typical of aromatic and antiaromatic classifications distinguished by their number of π-electrons, 4n+2 or 4n respectively.[4,5] According to Shaik and Hiberty, computational valence bond theory does give correct predictions for cyclobutadiene once ionic resonance structures are included in the calculation.[6] Early researchers such as Pauling used valence bond theory or molecular orbital theory based on what was most practical for the particular application.[7] The valency interaction formula method, VIF,[8−10] makes salient features of both qualitative VB and qualitative MO theories available in a unified approach.

In this paper, key chemical bonding motifs are examined using quantum mechanically derived molecular structural formulas. Resonance structures are compared to VIF pictures related by the two pictorial VIF rules. Unlike the resonance structures, VIF pictures as one-electron density operators can be used to predict the symmetries of aromatic and anti-aromatic rings according to the number of paired and unpaired electrons in the π-system. Due to the fact that VIF is a one-electron theory and the pictorial VIF rules are linear transformations, the VIF pictures have a closer relationship with natural bond orbitals,[11] NBOs, and natural resonance structures, NRS, than they do with the many-electron wave functions of valence bond theory. The correspondence between VIF pictures as one-electron density operators and as one-electron Hamiltonian operators allows the calculated energies of NBOs with respect to the VIF reference energy of $-1/2E_h$ to be interpreted in terms of valence shell electron pair repulsion (VSEPR)[12] theory.

II. Theory of Structural Covariance

The mathematical foundations for the VIF method were formulated by Sinanoğlu and presented in a series of five papers in 1984.[13] In the fourth of the five papers, "Structural Covariance of Graphs", Sinanoğlu shows how an algebraic structure such as a linear operator can be represented with a graph, G, and states that all $\{G, G', G'',...\}$ obtained by transforming the initial

* Author for correspondence. E-mail: aliaj@morris.umn.edu.

Valency Interaction Formulas to Predict Molecular Properties

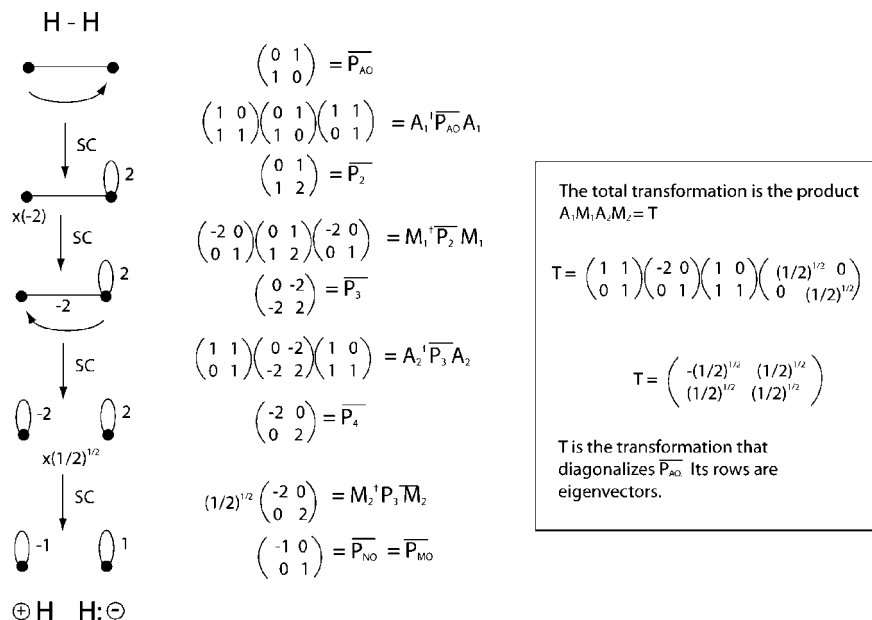*J. Phys. Chem. A, Vol. 112, No. 40, 2008* **9785**

Figure 1. (Left) Reduction of the VIF picture for H_2 molecule using the two VIF rules compared to major and minor resonance structures for hydrogen. (Center) Linear transformations corresponding to the application of the two pictorial rules. (Right box) Eigenvectors found as the product of transformations used to reduce the VIF picture.

linear basis frame by a transformation, S, in the general linear group will be termed "structurally covariant". The same paper later presents these transformations in terms of two pictorial rules that can be applied to the graphs. In the chemical applications that have followed, these pictorial rules have been referred to as the "VIF rules" and the graphs as "VIF pictures". Each member in a set of "structurally covariant" VIF pictures has the same number of positive, zero, and negative eigenvalues, i.e. has the same signature. These are enumerated in the level pattern index, LPI (n_+, n_0, n_-), where n_+ is the number of bonding orbitals, n_0 is the number of nonbonding orbitals, and n_- is the number of antibonding orbitals if the VIF represents a one-electron Hamiltonian operator or the orbital occupancy index, OOI(n_2, n_1, n_0), with n_2 as the number of doubly occupied orbitals, n_1 as the number of singly occupied orbitals, and n_0 as the number of unoccupied orbitals if the VIF represents a one-electron density operator (Alia 2007).

VIF Definitions and the Two Pictorial Rules. VIF pictures as effective one-electron density operators, $\bar{\rho}$, are drawn with respect to a reference electron density of one electron per orbital. $A^{\mu\mu}$ (indices the same), shown in eq 1 below, are valency points, dots in the VIF picture, and valency interactions, $A^{\mu\nu}$ ($\mu \neq \nu$) are all implicit even though only those with significant values of $\bar{P}_{\mu\nu} = (P_{\mu\nu} - 1 \cdot S_{\mu\nu})$, where $S_{\mu\nu}$ are elements of the overlap matrix, are explicitly shown in the VIF picture. Otherwise, $P_{\mu\nu} \approx 1 \cdot S_{\mu\nu}$ so $\bar{P}_{\mu\nu} \approx 0$ and no valency interaction is drawn in the VIF picture. Decision of which valency interactions to draw in a VIF picture is based on chemical intuition and can be tested using the two pictorial VIF rules.

$$\bar{\rho} = \bar{P}_{\mu\nu} A^{\mu\nu} = \bar{P}_{\mu\nu} |\phi^\mu\rangle\langle\phi^\nu| = (P_{\mu\nu} - 1 \cdot S_{\mu\nu})|\phi^\mu\rangle\langle\phi^\nu|$$

$$\text{with } A^{\mu\nu} = \left(\frac{|\phi^\mu\rangle\langle\phi^\nu| + |\phi^\nu\rangle\langle\phi^\mu|}{2} \right) \quad (1)$$

The summation convention implies summation over indices μ and ν in the expression for $\bar{\rho}$ in eq 1. If the VIF picture represents an effective one-electron Hamiltonian operator, $\bar{h}$, then $\bar{P}_{\mu\nu}$, is replaced by $\bar{h}_{\mu\nu} = (h_{\mu\nu} - \alpha \cdot S_{\mu\nu})$ where α is the reference energy. A convenient reference energy is $\alpha = -1/2$

E_h. Alia (2007) has shown that with a reference electron density of one electron per orbital and reference energy $-1/2$ E_h, VIF pictures as one-electron density operators or as one-electron Hamiltonian operators are frequently the same picture. Likewise, $\bar{h}_{\mu\nu} = 0$ implies $h_{\mu\nu} = \alpha \cdot S_{\mu\nu}$ so all valency interactions are implicit but only the chemically significant ones are drawn. The VIF picture thus has correct transformational properties for these operators in a valence orbital representation for a given molecule (Alia 2007). Valency points may have attached loops with loop constant and valency interactions may have strength κ. One draws loops and valency interactions in the VIF picture only for relevant values of $\xi = \bar{h}_{\mu\mu}/\beta_o$, $\kappa = \bar{h}_{\mu\nu}/\beta_o$ or likewise $\xi = \bar{P}_{\mu\mu}/\beta_o$, $\kappa = \bar{P}_{\mu\nu}/\beta_o$.

Loop and line constants, and κ, are unitless, and β_o is chosen so that $\kappa = 1$ is the default value. Valency interaction strengths are therefore relative, and the VIF picture can be drawn without evaluation of integrals corresponding to $P_{\mu\nu}$ or $h_{\mu\nu}$. Intra-atomic values of these are based on electron configurations in atoms or VOIEs respectively and tentative relative interatomic valency interaction strengths are based on a presumed molecular geometry the quantum-based properties of which are to be tested using the two pictorial rules described below.

1. Multiplication rule: A valency point ($A^{\mu\mu}$) may be multiplied by a nonzero constant. All constants (κ) of valency interactions attached to $A^{\mu\mu}$ are then multiplied by this nonzero constant. If $A^{\mu\mu}$ has a loop, its constant, is multiplied by the square of the nonzero constant.

2. Addition rule: A valency point ($A^{\mu\mu}$) may be "lifted" and superimposed on another valency point ($A^{\nu\nu}$). All valency interactions (VI) and loops attached to $A^{\mu\mu}$ are carried along. Constants, and κ, of superimposed loops and VI respectively add. If $A^{\mu\mu}$ and $A^{\nu\nu}$ are connected by a VI of strength κ, this VI curls up to form a loop with strength 2κ on $A^{\nu\nu}$. If $A^{\nu\nu}$ already had a loop, the curled up loop superimposes this original loop and the value 2κ is added to the original loop constant, on $A^{\nu\nu}$. $A^{\mu\mu}$, the VI attached to it, and loop if it has one, are not removed, they remain as if "chalk marks" left behind.

These rules are now demonstrated in VIF pictures for a hydrogen molecule and compared side-by-side with the corre-

sponding linear transformations applied to the valence-space one-electron charge-density bond-order matrix, $\bar{P}_{AO}$, transforming it from an atomic orbital, AO, representation to a delocalized molecular or natural orbital representation, $\bar{P}_{MO}$ or $\bar{P}_{NO}$. The line over the top indicates that each matrix has elements calculated with respect to a reference electron density of one electron per orbital.

Demonstration of the VIF Rules for the H_2 Molecule. VIF pictures for the H_2 molecule are shown in Figure 1. There is a valency point, $A^{\mu\mu}$, for each hydrogen 1s orbital. With a reference electron density of one electron per orbital, these have no loops. $P_{\mu\mu} = 1 \cdot S_{\mu\mu} = 1$ so $\overline{P_{\mu\mu}}/\beta_o = \beta = \xi = 0$. The line that connects the two valency points represents interaction between these orbitals and is a valency interaction, $\overline{P_{\mu\nu}}/\beta_o = \kappa = 1$ by default.

Application of the pictorial VIF rules and their corresponding linear transformations are also shown in Figure 1. As indicated in the previous section, a valency point may be multiplied by a nonzero constant in which case the valency interactions emanating from it are multiplied by this constant (**multiplication rule**) or a valency point may be superimposed on another valency point bringing its valency interactions with it (**addition rule**). Applying the addition rule, the strengths of superimposed interactions add. Notice that in Figure 1, the addition rule is used first. When the left valency point is superimposed on the right one, valency interactions are superimposed, and the valency interaction, in this case with default value $\kappa = 1$, curls up forming a loop of strength $2\kappa = 2 = \xi_R$. The original left valency point and valency interaction remain like chalk marks. The left valency point in Figure 1 is now multiplied by -2 so that $\kappa = -2$. Using the addition rule again, the right valency point is superimposed on the left. The $\xi = 2$ loop stretches over the $\kappa = -2$ interaction, canceling it. Simultaneously, the line strength $\kappa = -2$ curls up to form a loop with strength -4 on the left valency point. The right valency point loop was carried along and superimposed on the left valency point, making its overall strength $\xi_L = -4 + 2 = -2$. Compare the VIF pictures on the left of Figure 1 with the linear transformations on the right. The loop strengths are now normalized by multiplication by $(1/2)^{1/2}$, giving $\xi_L = -1$ and $\xi_R = 1$. $\bar{P}_{AO}$ has been diagonalized to $\bar{P}_{MO}$ or $\bar{P}_{NO}$ by application of linear transformations. From the point of view of a basis frame in which $\bar{P}_{MO}$ and/or $\bar{P}_{NO}$ are diagonal, there is now one valency point, $A^{\mu\mu}$, for each delocalized orbital, molecular or natural. Adding back the reference electron density of one electron per orbital indicates one doubly occupied and one unoccupied orbital, OOI(1,0,1). VIF pictures related by these pictorial rules, linear transformations, make a set of structurally covariant graphs indicated by "**sc**" in Figure 1.

Three Interpretations of Structurally Covariant VIF Pictures

Interpretation 1. Structurally covariant graphs (VIF pictures) may represent the same operator in different linearly related basis frames as is the case when the VIF picture is simplified using the two pictorial rules to find the level pattern index, LPI, or orbital occupancy index, OOI.

Interpretation 2. Structurally covariant graphs may represent operators for different molecular species in the same basis frame. For example, the graphs may represent molecular isomers or reactants, transition structures, and products grouped into the same equivalence class by use of the VIF rules. Sinanoğlu anticipates species grouped into the same equivalence class to have "qualitatively the same thermicity" (Sinanoğlu, 13d).
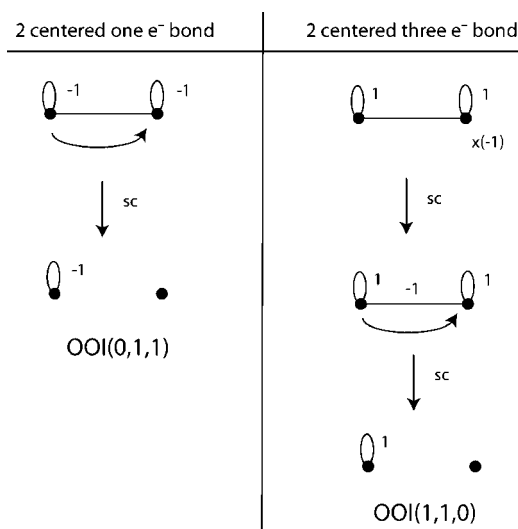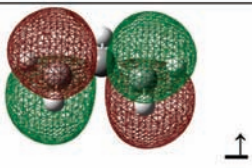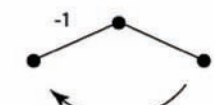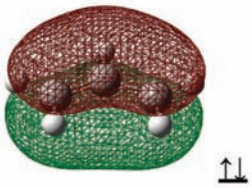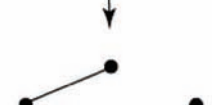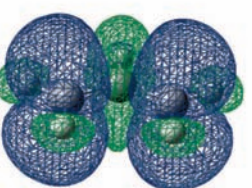

Figure 2. (Left) VIF pictures for a two-centered one-electron bond as in H_2^+. (Right) VIF pictures for a two-centered three-electron bond, π-bonds in triplet O_2 for example.

Interpretation 3. The same VIF picture can also represent different types of operators, one-electron Hamiltonian or one-electron density for example (Alia 2007).

The VIF pictures in Figure 1 represent one-electron density operators so the positive and negative loops in the bottom picture represent a doubly occupied and an unoccupied orbital, respectively, OOI(1,0,1) in an nonlocalized natural orbital or molecular orbital frame. The same set of structurally covariant VIF pictures can correspond to a localized basis frame linearly related to the delocalized frame (**interpretation 1**). The VIF picture at the bottom of Figure 1 can therefore represent a minor natural resonance structure of the hydrogen molecule while the initial VIF picture at the top of Figure 1 represents the major natural resonance structure. The other minor resonance structure can easily be represented using the VIF rules in a way similar to the first one. If the VIF pictures in Figure 1 represent one-electron Hamiltonian operators instead of one-electron density operators (**interpretation 3**), then the positive loop and negative loops in the bottom VIF picture in Figure 1 correspond to bonding and antibonding molecular orbitals with respect to a reference energy of $-1/2$ E_h, LPI(1,0,1). Figure 1 indicates how application of the VIF rules is analogous to matrix diagonalization. The product of the linear transformations used is the eigenvector matrix for H_2 (**interpretation 1**). Because VIF pictures are frequently reduced to pictures containing several pairs of valency points connected only to each other, each with LPI(1,0,1) and/or OOI(1,0,1), these results for H_2 are easily transferred to other examples. From the energetic point of view, they offer a chemical picture in which localized bond orbitals[11] are accompanied by localized antibonding orbitals analogous to an NBO representation.

Other possibilities for two-centered bonds are the 2c/1e$^-$ bond like in the H_2^+ cation and 2c/3e$^-$ electron bond of which the O_2 molecule π-bonds are examples.[14] These cases are easily represented using VIF pictures as one-electron density operators. See Figure 2. The disconnected valency points with no loops in the reduced pictures represent singly occupied orbitals. H_2^+ has one singly occupied orbital and one unoccupied orbital, OOI(0,1,1), while each of the ground-state triplet O_2 π-bonds have a doubly occupied π-orbital and a singly occupied π^*-orbital, OOI(1,1,0). Taken together, these comprise Pauling's two-centered three-electron bond (Pauling 1931, page 1385).

TABLE 1: VIF Pictures for the Allyl Radical π-System Compared with Resonance Structures and Contour Diagrams for Computed Molecular Orbitals and Spin Density

Note that two-centered four-electron bonds have equal numbers of bonding and antibonding electrons and so do not occur.

In the most commonly used types of structural formulas, Lewis structures, bond connectivity indicates places where electron pairs are likely found. VIF pictures to which the pictorial rules have been applied show this type of connectivity and, as one-electron density operators, they show where electron pairs or radical electrons are likely found. VIF pictures for the allyl radical π-system are shown in Table 1. Once again, pictures related by the pictorial rules are structurally covariant, and therefore, each picture corresponds to the same orbital occupancy index, OOI, or level pattern index, LPI. Interpreted as one-electron density operators, the VIF pictures at the bottom of Table 1 indicate the high probability that the unpaired electron will be found on the terminal carbon atom. All of the pictures in Table 1 correspond to the same OOI(1,1,1), one doubly occupied orbital, one singly occupied orbital, and one unoccupied orbital. This is true whether the basis frame is a delocalized frame, MO for example, or a localized one, such as NBO.

What is essential is that VIF pictures as one-electron density operators for molecules, molecular ions, or assemblies of reacting molecules conform to the correct number of valence electrons and the correct spin multiplicity.

As will be shown in the following sections of this paper, finding the VIF pictures that do conform to the molecule's known number of valence electrons and spin-multiplicity provides further insight into the molecule's structure and reactivity. For example, it will be shown that VIF pictures that conform to the correct number of electrons for cyclic π-systems predict the symmetry of the ring. VIF pictures as one-electron density operators have a close relationship to natural orbital, NO, and natural bond orbital, NBO, representations. VIF pictures are compared to lone pair and bond pair NBOs. In cases where the same VIF pictures represent both one-electron density operators and one-electron Hamiltonian operators, VSEPR can be used in the comparison of computed NBO energies with results from the VIF. These properties are demonstrated for a variety of examples that follow.

III. Computational Details

Computations were performed using the GW03 package.[15] Molecular geometries were optimized using the B3LYP/6-311++Gdp level of theory. Input files were made and results viewed with the help of the GaussView graphical interface. Various NBO options were utilized.

IV. Applications

Three-Centered Bond in the Allyl π-System. Three-centered bonds are an important structural motif, helpful in understanding the properties of a variety of molecules and ions, from the three-centered four-electron carbonyl π-system bonds endowing carboxylic acids with their distinctive acid character, to the delocalized carbonyl π-system and nitrogen lone pair of amides, resulting in their planar geometry and rotational barrier around the carbonyl C−N bond, to electron-deficient species such as carbocations and boranes. In this section, allyl radical, anion, and cation cases are presented as the simplest three-centered bonding examples. More complicated examples follow in the later sections of this paper.
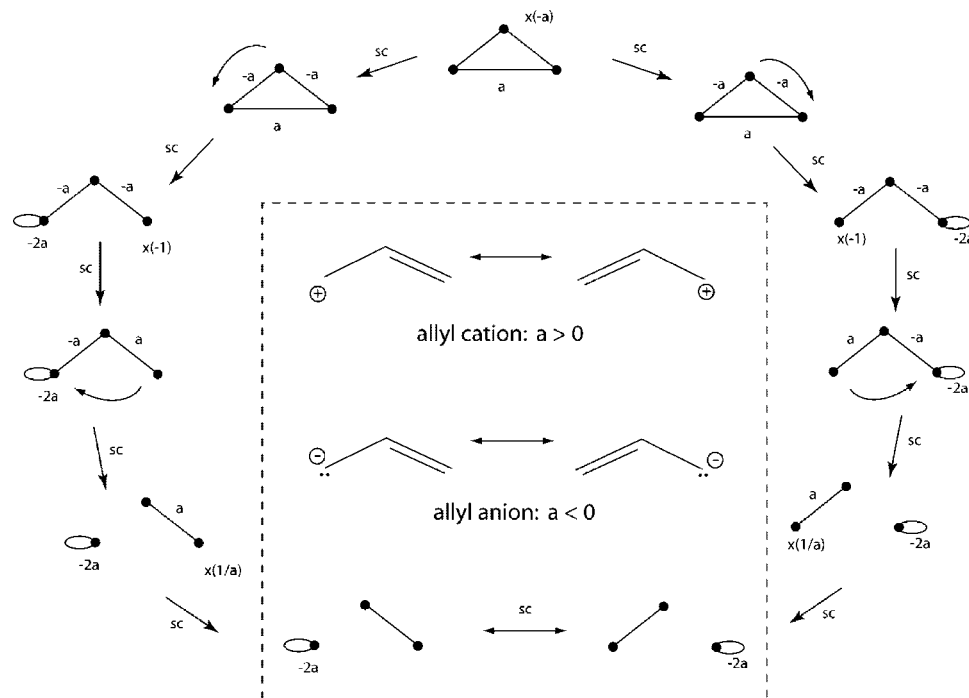
Figure 3. Relevance of interaction between terminal π-orbitals in the allyl π-system is tested using the VIF rules. This interaction with a strength of a is found to be relevant for the allyl anion for which a has a negative value and the allyl cation for which a is positive. These pictures related by the VIF rules are structurally covariant and consistent with resonance structures for these species.

VIF pictures for the allyl radical π-system are shown in Table 1 along with resonance structures and contour plots of the occupied π-molecular orbitals and a spin density plot. The initial VIF pictures show the interactions between the carbon p-orbital on the central carbon and those on each of the two terminal carbons are significant while the interaction between the π-system p-orbitals on the terminal carbons is considered insignificant, $\bar{P}_{13} = (P_{13} - 1 \cdot S_{13}) \approx 0$, where the subscripts 1 and 3 designate p-orbitals on the terminal carbon atoms.

The VIF rules applied in Table 1 are used to find structurally covariant VIF pictures with a pair of valency points connected only to each other indicating one doubly and one unoccupied orbital, as for the H_2 molecule, and also a detached valency point with no loop indicating a singly occupied orbital, that is, an unpaired electron as is expected for a radical species. All VIF pictures in Table 1 are consistent with orbital occupancy OOI(1,1,1). The reduced VIF pictures taken as one-electron density operators in a localized orbital representation show the singly occupied orbital to be centered on the terminal carbon atoms in agreement with all of the other pictures and methods displayed in Table 1. The same VIF pictures interpreted as one-electron Hamiltonian operators indicate one bonding molecular orbital, one nonbonding molecular orbital and one antibonding molecular orbital with respect to the energy of a carbon 2p orbital, LPI(1, 1, 1). This is exactly as one would expect from a simple Hückel MO approach with no interaction between the terminal p-orbitals in the π-system. Unlike the Hückel MO method, all overlaps are implicit in the VIF method since $\bar{P}_{\mu v} = (P_{\mu v} - 1 \cdot S_{\mu v})$ and the OOI and LPI are invariant under linear transformations.

In Figure 3 the significance of an interaction between the p-orbitals on the two terminal carbon atoms is tested by giving the corresponding valency interaction a strength of a. It is shown in Figure 3 that the interaction of strength a results in two structurally covariant "resonance" structures each including a line segment giving one doubly occupied and one unoccupied orbital as before but also a detached valency point with a loop

of strength $-2a$. As before, the detached valency point has ended up on a terminal carbon atom, but whether it corresponds to a pair of electrons or an empty orbital depends on whether a is greater or less than zero. If $a > 0$, then OOI(1, 0, 2) and the species described is the allyl cation. If $a < 0$, then OOI(2, 0, 1) and the VIF picture corresponds to the allyl anion.

Computed elements, $P_{\mu v}$, support a negative value of a in the allyl anion and a positive value of a in the allyl cation. Density elements for a set of interacting 2p π-type natural atomic orbitals, NAOs, in the allyl anion were calculated by Weinhold (2005, page 33) and are shown in eq 2.

$$D^{(\text{true})} = \begin{pmatrix} 1.4694 & 0.7061 & -0.4650 \\ 0.7061 & 0.9927 & 0.7061 \\ -.4650 & 0.7061 & 1.4694 \end{pmatrix} \quad (2)$$

The negative values in the top right and lower left correspond to negative values of a. The qualitative conclusions from the VIF picture as a one-electron density operator match the computed density elements. If $a > 0$, then OOI(1, 0, 2) results. If $a = 1$, the default value, as would be expected for the cyclopropenyl cation, then we expect the molecular geometry to be D_{3h}. The cyclopropenyl cation has the simplest possible $4n+2$ aromatic π-system.

Minor resonance structures for allyl radical, anion, and cation are compared with their corresponding VIF pictures found using the two VIF rules in Figure 4. Minor resonance structures are useful because they can give insight into chemical reactivity. Rules for pushing pairs of electrons allow one to predict bond breaking and formation during a chemical reaction consistent with the octet rule. Lewis structures are not reliable in predicting numbers of paired and unpaired electrons, as the examples of O_2 and cyclobutadiene indicate. The VIF method gives correct predictions for both of these examples (Alia 2007 and this paper). Structurally covariant VIF pictures allow prediction of bond breaking and formation, processes that preserve the number of doubly, singly, and unoccupied orbitals.
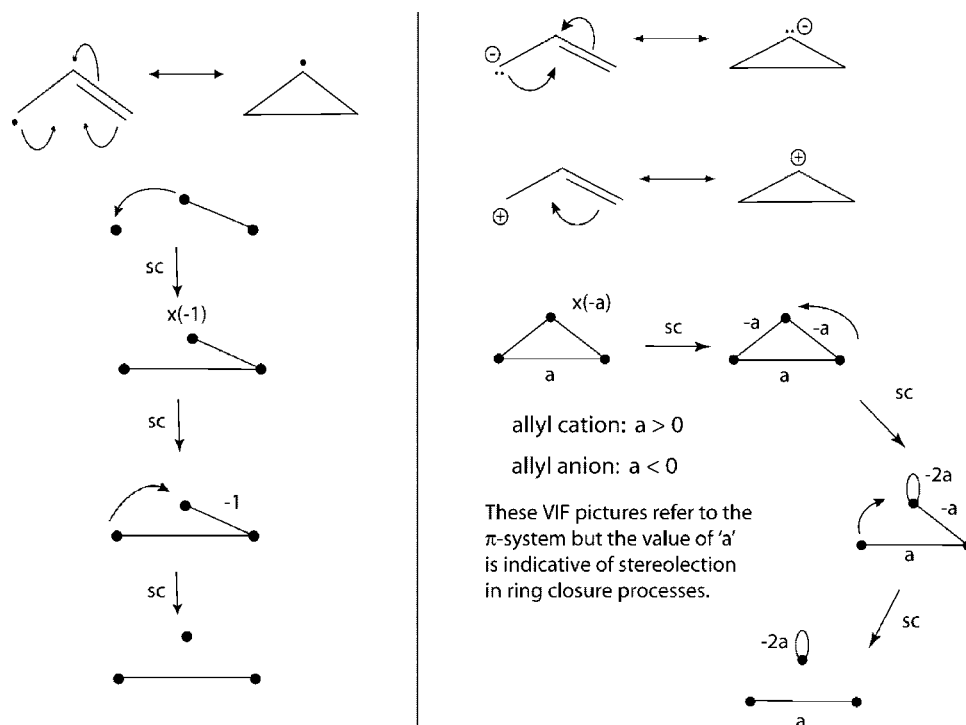
Figure 4. (Left) VIF rules used to generate structurally covariant pictures corresponding to the ring closure of the allyl radical. (Right) VIF rules used to generate structurally covariant pictures corresponding to the ring closure of the allyl cation and anion. The sign of *a* depends on whether the cation or anion is being described and consistent with the respective disrotatory and conrotatory pathways for these processes.

The negative value of *a* for the allyl anion indicates that the p-orbital contributions on the terminal carbons in the highest occupied molecular orbital, HOMO, are out of phase and thus have a negative interaction between them. A conrotatory transition structure is therefore required to form positive overlap in σ-bond formation during ring closure preserving the symmetry of this orbital.[16] The two electrons involved in this ring closure are those in the allyl anion HOMO with its C_2 axis of rotation. The remaining two π-electrons form the lone pair in the cyclopropyl anion specified by the loop with $\xi = -2a$ in Figure 4. Ring closure for the allyl cation would preserve the positive interaction with $a > 0$ and OOI through its disrotatory ring closure as expected from symmetry of the π-HOMO for this $4n+2$ π-electron system. Since $a = 0$ for the allyl radical, this species is not expected to have stereoselectivity strongly influenced by orbital control.

In this section we have presented the VIF description of three-centered bonding types with two, three, and four electrons. The three-centered four-electron bond (3c/4e⁻) as in the allyl anion has higher π-electron probability on the terminal carbon atoms and can undergo ring closure through a conrotatory process, maintaining OOI(2,0,1). The three-centered two-electron, 3c/2e⁻, bond describes the π-systems in the allyl cation and cyclopropenyl cation which is also the simplest example of a $4n+2$ aromatic species. Structurally covariant VIF pictures found using the two VIF rules, thereby maintaining the LPI or OOI, are consistent with molecule or ion charge distribution and selectivity in concerted ring closure reactions.

Singlet and Triplet States of Cyclobutadiene. Valency interaction formulas for the cyclobutadiene π-system are shown in Figure 5. The pictures on the left assume that the nearest-neighbor interactions are all equal. This corresponds to D_{4h} symmetry. The VIF rules applied to this picture indicate that it is structurally covariant with two singly occupied orbitals, OOI(1,2,1), as shown by the two detached valency points in the picture in the lower left corner of Figure 5. D_{4h} is the

symmetry for the cyclobutadiene triplet state according to Hund's rule. The VIF pictures on the right side of Figure 5 allow for the possibility that cyclobutadiene has a rectangular shape with distinct alternating single and double bonds around the ring. Notice that it is not possible to get from the pictures on the left side of Figure 5 to those on the right by using the VIF rules. The VIF pictures on the right are *not* structurally covariant with those on the left. Application of the VIF rules to the pictures on the right results in two line segments, (bottom right picture) one with a strength of −1, the other a strength of $1 - a^2$. With a rectangular, D_{2h}, symmetry $a \neq 1$, OOI(2,0,2) results. There are two doubly occupied and two unoccupied π-orbitals therefore the electronic state is a singlet. Distortion from D_{4h} to D_{2h} to break degeneracy and stabilize a pair of electrons is a well-known phenomenon and an example of a Jahn−Teller distortion. When the VIF pictures in Figure 5 are interpreted as one-electron Hamiltonian operators with LPI(1,2,1) for the D_{4h} geometry, the two detached valency points that result correspond to a pair of degenerate nonbonding molecular orbitals at the reference energy, α_{C2p}, each singly occupied. Distortion to the rectangular geometry, D_{2h} symmetry, results in LPI(2, 0, 2). See Figure 5. The electrons previously in the nonbonding orbitals are now stabilized in a bonding orbital lower in energy than the α_{C2p} reference energy.

Cyclopentadienyl Species. Cyclopentadienyl anion, radical, and cation have symmetries that can be predicted based on their number of π-electrons using VIF pictures as one-electron density operators. Figure 6 (top) shows VIF pictures for the cyclopentadienyl anion. All of the interactions around the five-membered ring are equal, corresponding to D_{5h} symmetry. The VIF rules are applied and two fragments result, a pair of valency points connected only to each other and a set of three valency points connected in a triangle with one negative interaction. Both of these types of VIF fragments have been discussed in this paper already. The orbital occupancy index for cyclopentadienyl anion with its D_{5h} symmetry is OOI(3,0,2). The three electron pairs
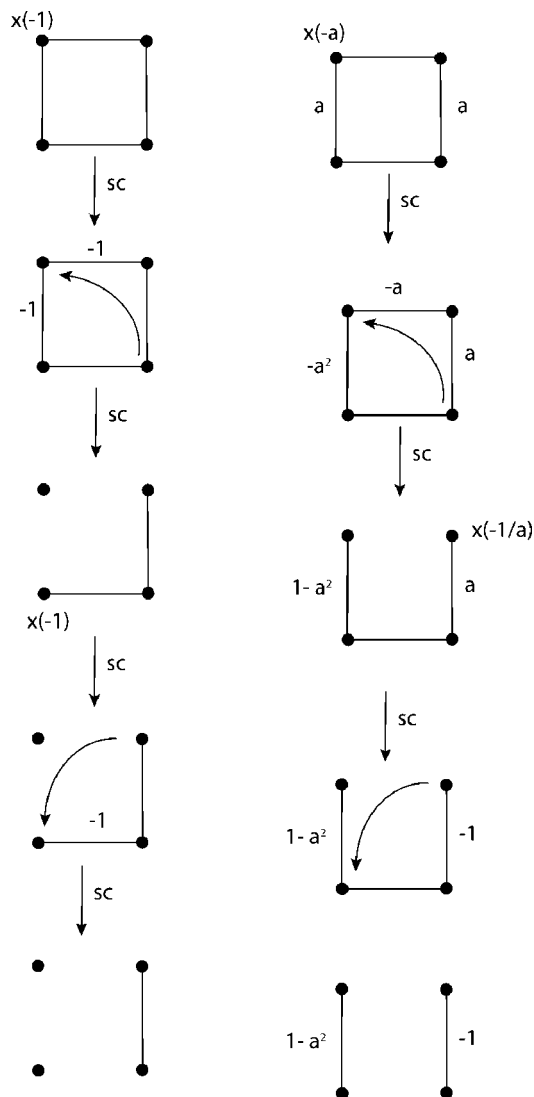
Figure 5. (Left) VIF rules used to generate structurally covariant pictures corresponding to the cyclobutadiene π-system with D_{4h} symmetry. The two disconnected valency points in the bottom left picture indicate two singly occupied orbitals and a triplet ground-state for this geometry. (Right) The constant a is used to test the effect of alternating interaction strengths around the ring. Structures with $a \neq 1$ correspond to a singlet state with two doubly and two unoccupied valence π-orbitals.

Figure 6. (Top) VIF pictures for cyclopentadienyl anion π-system. All interactions around the ring are equal. This is consistent with D_{5h} symmetry. Application of the VIF rules leads to three doubly occupied orbitals, no singly occupied orbitals, and two unoccupied orbitals, OOI (3,0,2). (Middle) Neglect of one of the interactions around the ring conforms to the correct number of doubly, singly, and unoccupied orbitals for the cyclopentadienyl radical and also predicts its C_{2v} symmetry. (Bottom) One negative interaction leads to OOI(2,0,3) required for the cyclopentadienyl cation and predicts it to have C_{2v} symmetry.

result as is necessary for this anion's π-system, and the D_{5h} symmetry is consistent with aromatic behavior of this $4n+2$ electron aromatic species.

The π-system VIF for the cyclopentadienyl radical must result in OOI(2,1,2), consistent with one unpaired electron. A VIF picture that meets this requirement is shown in Figure 6 (middle). In this picture the valency interaction between the two bottom valency points has been set to zero. The VIF rules are applied, and a single detached valency point results, indicating, the singly occupied orbital consistent with a radical. The removal of the bottom valency interaction indicates that the cyclopentadienyl radical does not have D_{5h} symmetry but C_{2v}. This prediction is supported by geometry optimization on the B3LYP/6-311++Gdp level of theory. See Figure 7. Examination of π-system density elements calculated using the minimal basis HF/STO-3G, also shown in Figure 7, supports our setting the bottom density element to zero in this VIF picture.

The π-system VIF for the cyclopentadienyl cation must have OOI(2,0,3) which results if one of the valency interactions
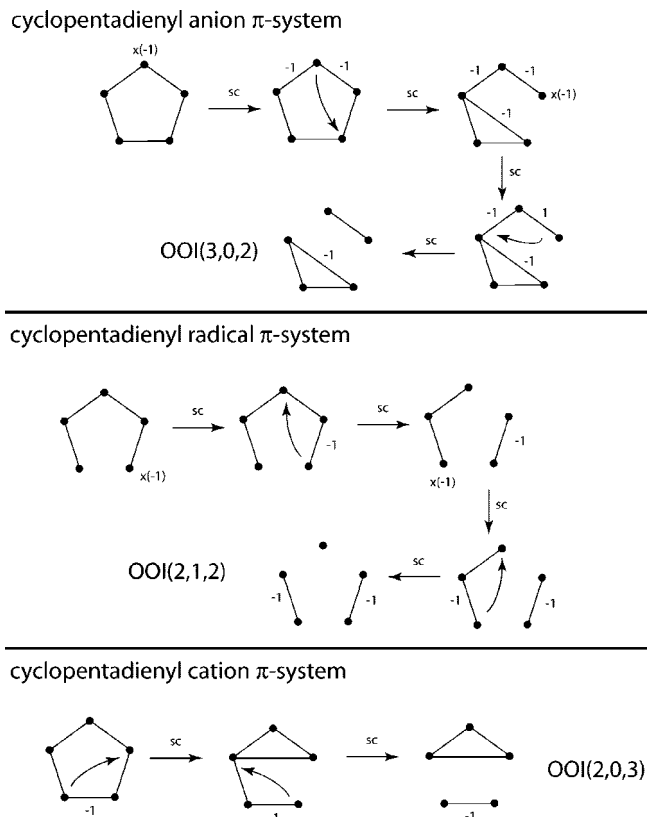
around the ring has a negative value. This is consistent with C_{2v} symmetry and the geometric distortion expected for an antiaromatic $4n$ π-electron ring system. Both the C_{2v} symmetry and the negative density element are supported by B3LYP/6-311++Gdp and HF/STO-3G calculations, respectively. See Figure 7.

π-Distortivity of Benzene. The benzene molecule's shape is known to be easily distorted between D_{6h} and D_{3h} symmetries.[17] The π-system VIF pictures for benzene shown in Figure 8 describe both D_{6h} benzene and distorted D_{3h} benzene. For the usual D_{6h} benzene, the constant, a, would be equal to one. Reduction of the VIF picture shown in Figure 8 indicates that if $a > -1$, then the picture results in OOI(3,03) and LPI(3,0,3). A very wide span of distortions is described by $a > -1$. This is consistent with the fact that benzene is easily distorted.

Benzyl Radicals. The unpaired electron in the benzyl radical is delocalized throughout the π-system and has the highest probability of being observed in the ortho, para, or benzylic positions. VIF pictures as one-electron density operators for the benzyl radical π-system are shown in Figure 9. The VIF pictures with the singly occupied localized orbital in ortho, para, or benzylic position are related by the VIF rules and thus structurally covariant, all with the same OOI(3,1,3). All of these pictures are also related to the SOMO which places spin density in the ortho, para, and benzylic positions. The benzyl radical SOMO is shown in Figure 10.
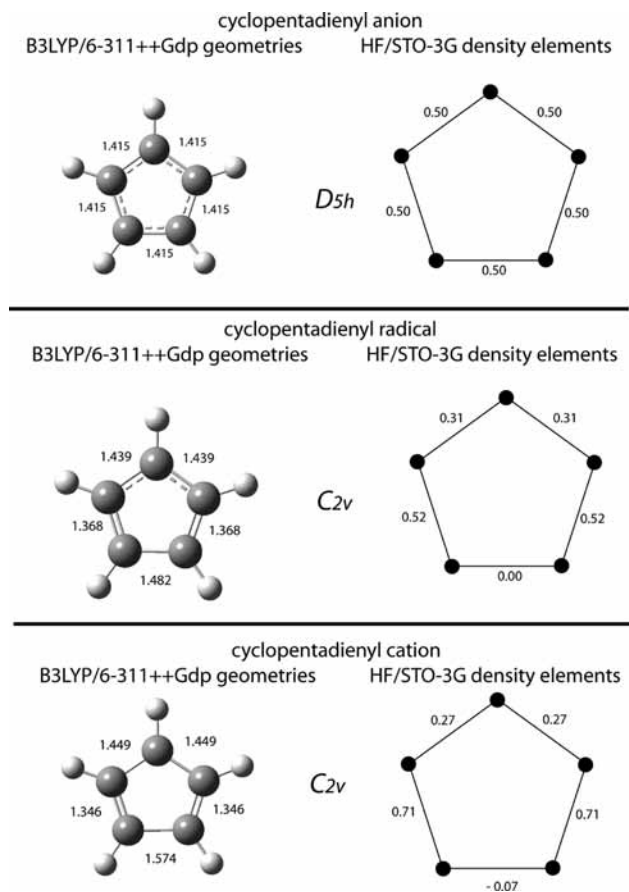
Valency Interaction Formulas to Predict Molecular Properties

J. Phys. Chem. A, Vol. 112, No. 40, 2008 **9791**

Figure 7. Predictions made in Figure 6are supported by optimized geometries calculated using B3LYP 6-311++Gdp and density elements calculated using HF STO-3G.

Figure 8. (Top) π-Distortivity of the benzene molecule is tested. All values of a greater than -1 correspond to three doubly occupied bonding π-molecular orbitals and are consistent with easy distortion of the ring.

H-Bridging Bonds in Diborane. Now after seeing how the VIF method is applied in a number of ring-system bonding situations, we turn to diborane to apply these ideas further. Diborane provides a historically important example with its two three-center two-electron H-bridging bonds. A common way of representing bridging bonds is the τ-bridged representation, Figure 11 (top).[18] Lipsomb's contribution toward understanding borohydrides and development of the theory of the 3c/2e$^-$ bond was recognized when he was awarded the 1976 Nobel Prize in chemistry "for his studies on the structure of boranes illuminating problems of chemical bonding".[19] Weinhold (2005) demonstrates insights that can be gained by applying the NBO method to boranes and other examples with 3c/2e$^-$ bonds. According to Weinhold, "the three-centered bonds provide a genuinely new and necessary "building-block" of the Lewis-structure concept, if the accustomed accuracy of the concept is to be preserved for electron-deficient compounds."

The NBO method demonstrates that τ-bonds are stabilized by donor−acceptor delocalization involving the τ-antibonding orbitals. Such delocalizing interactions are significant to the accurate portrayal of diborane's τ-bonds using the VIF method. Figure 11 shows VIF pictures with (*right*) and without (*left*) interactions drawn between the boron atoms and between the bridging bonds. Loops indicating the electron deficiency of boron do not change our results and are neglected for the sake of a simpler presentation. Application of the VIF-rules results in two 3c/2e$^-$ bonds consistent with the known number of valence electrons for diboranes. If the interactions between the bridging bonds is not included in the original VIF picture, a six-membered ring results, connecting the boron valency points
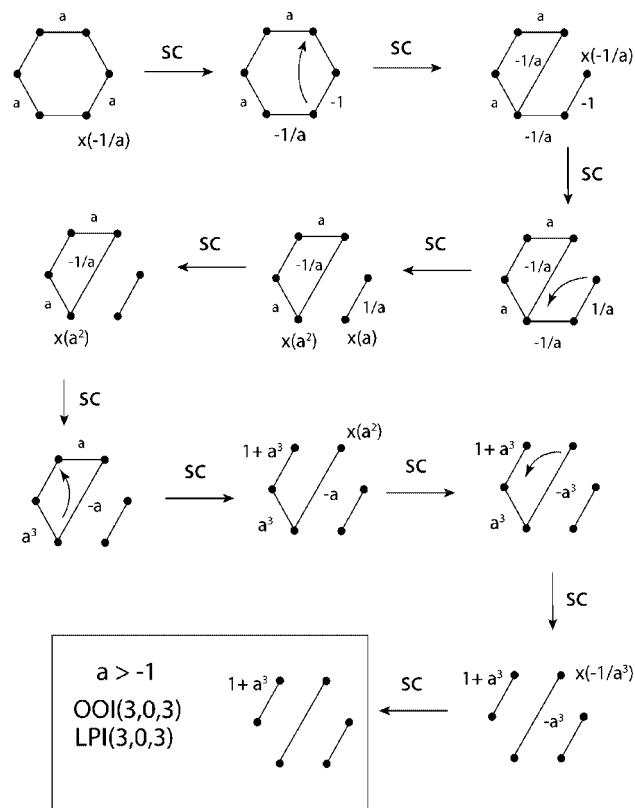
and bridging hydrogen atoms. This is analogous to the benzene π-system giving a total OOI(7,0,7) for diborane. Diborane with 12 valence electrons cannot have 7 doubly occupied valence orbitals. This picture also implies that a dicarbane molecule with bridging hydrogen atoms would exist which is obviously incorrect. If the correct VIF picture for diborane, Figure 11 *right*, is taken to be a one-electron Hamiltonian operator with a reference energy $-1/2\ E_h$, the level pattern index, LPI(6,0,8) is in good agreement with the B3LYP/6-311++Gdp valence NBO energies in E_h,

$$-0.717, -0.717, -0.592, -0.592, -0.592, -0.592$$
$$0.343, 0.343, 0.592, 0.592, 0.680, 0.680, 0.680, 0.680$$

Six valence orbitals are lower in energy than $-1/2\ E_h$, and eight are higher in energy than $-1/2\ E_h$, consistent with the LPI deduced using the VIF method.

VIF Applied to Some Common Functional Groups. We now turn to some common functional groups from organic chemistry in order to demonstrate how structurally covariant VIF pictures as one-electron density operators closely match the bond-pair, lone-pair bonding scheme for these molecules, to demonstrate the use of electronegativity loops, and to highlight the difference in behavior between lone pair orbitals as part of a σ-system and those as part of a π-system subject by varying degrees to VSEPR effects.

Ethanoic acid and acetamide are shown in Table 2 as examples of how acid an amide functional groups are described using VIF pictures as one-electron density operators. The results would be similar if a carbon chain were attached instead of the methyl group. It is crucial to account for delocalization of the p-hydroxyl or amino lone pair into the carbonyl π-system in these cases by using sp^2 hybridization on the involved atoms.
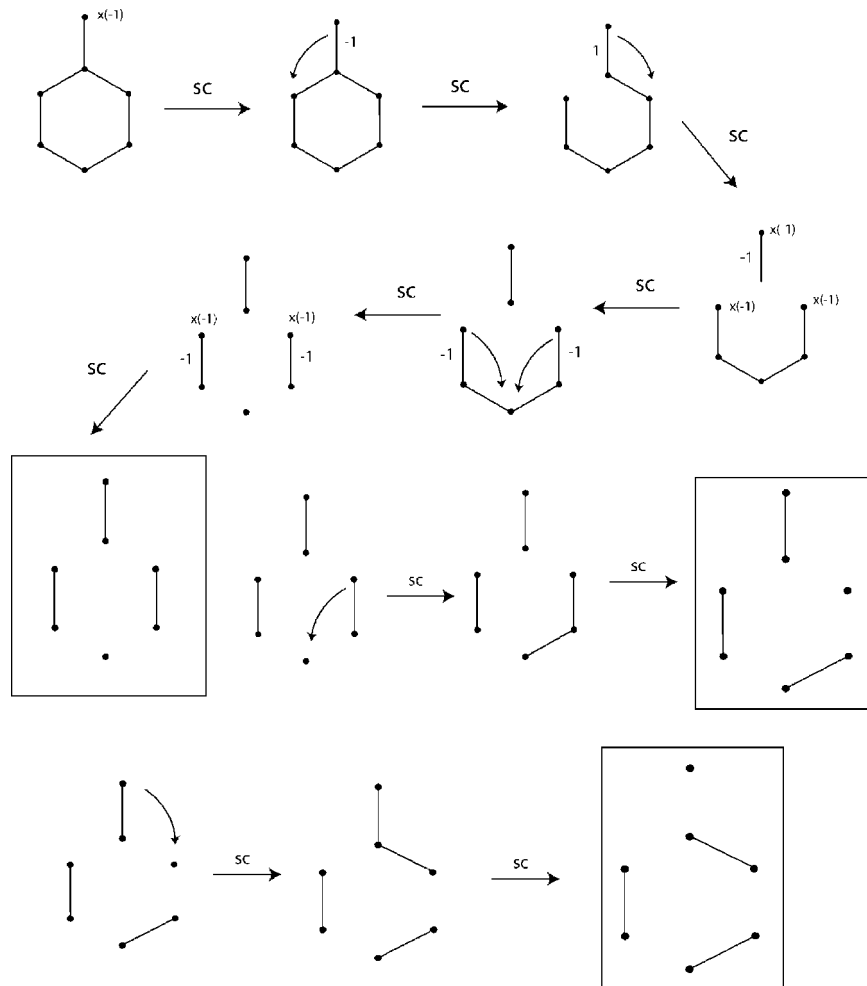
Figure 9. Structurally covariant VIF pictures for the benzyl radical π-system indicate that the radical electron is likely to be found in the benzyl, ortho and para locations.
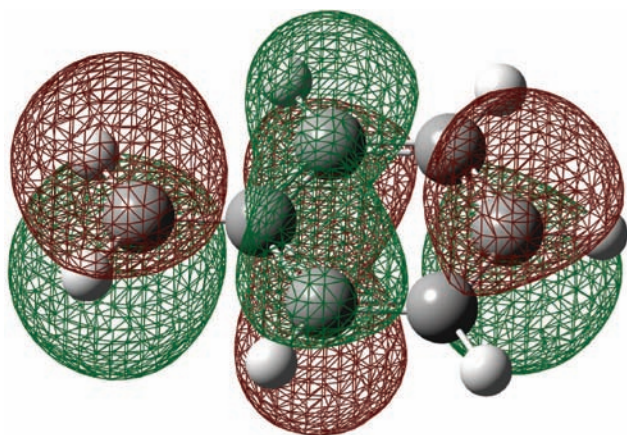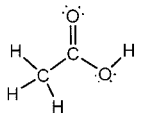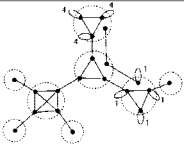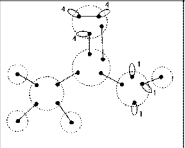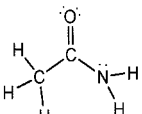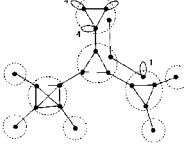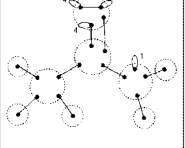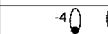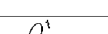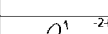

Figure 10. Benzyl radical SOMO calculated using B3LYP 6-311++Gdp supports the prediction that the radical electron has probabilities of being found in benzyl, meta, and para positions.

Otherwise, OOI will not match the correct number of valence electrons in these cases. The π-systems are therefore examples of 3c/4e⁻ bonds. Electronegativity loops for VIF pictures as one-electron density operators are calculated according to the hybridization of the atom in question. For sp^n hybrids $\alpha_{sp^n} = (\alpha_s + n\alpha_p)/(n + 1)$ and $\beta_{sp^n} = (\alpha_s - \alpha_p)/(n + 1)$. Loop constants are then found by subtracting the reference electron density of one electron per orbital and normalizing the intrahybrid interactions using the β value (Alia 2007).

The carbonyl oxygen contributes one electron to the C—O π-bond so three 2p electrons remain in the two 2p orbitals to be used in the sp^2 hybrid orbitals, and electronegativity loops for the σ-valency points of the carbonyl oxygen in each case have a loop constant = 4 calculated as follows. $\alpha_{Osp2} = [2 + 2(3/2)]/(2 + 1) = 5/3$, $\beta_{Osp2} = [2 - (3/2)]/(2 + 1) = 1/6$, and so $\xi_{Osp2} = ((5/3 - 1)/(1/6)) = 4$. The hydroxyl oxygen and amide nitrogen contribute a lone pair, two electrons, to the π-system. They therefore have electronegativity loop constants of 1 on their unhybridized 2p orbitals after subtraction of the reference of one electron per orbital. The σ-system loops for the hydroxyl oxygen are calculated as follows. $\alpha_{Osp2} = [2 + 2(2/2)]/(2 + 1) = 4/3$, $\beta_{Osp2} = [2 - (2/2)]/(2 + 1) = 1/3$, and so $\xi_{Osp2} = [(4/3) - 1]/(1/3) = 1$. Using the same method, the sp^2 orbitals for the amide nitrogen have no loops on their valency points, $\alpha_{Nsp2} = [2 + 2(1/2)]/(2 + 1) = 1$, $\beta_{Nsp2} = [2 - (1/2)]/(2 + 1) = 1/2$, and so $\xi_{Nsp2} = [1 - 1]/(1/2) = 0$. Both the VIF for ethanoic acid and acetamide are reduced using the pictorial rules to give pictures that are easily interpreted in terms of the lone pairs and bond pairs in each molecule. This is not the case if delocalization of lone pairs into the carbonyl π-bond is not accounted for by use of sp^2 hybridization which also corresponds to the correct planar geometry of these functional groups. These VIF pictures predict molecular geometries that have O—H and N—H bonds coplanar with the carbonyl group consistent with chemical knowledge, the theory of resonance, and geometry optimizations carried out at the B3LYP 6-311++Gdp level.

Valency Interaction Formulas to Predict Molecular Properties

J. Phys. Chem. A, Vol. 112, No. 40, 2008 **9793**

TABLE 2: Lewis Structures, VIF Pictures, Reduced VIF Pictures, and OOI for Acetamide and Acetic Acid and Some Resulting VIF Fragments[a]

species	VIF	Reduced VIF	OOI
			12, 0, 8
			12, 0, 9
Carbonyl oxygen lone pair fragment			**2, 0, 0**
C-O σ-bond fragment			**1, 0, 1**
O-H σ-bond fragment			**1, 0, 1**

[a] The VIF pictures indicate delocalization of lone pair electrons on the hydroxyl oxygen and nitrogen respectively. The π-systems for these molecules give further examples of four-electron three-center bonds, and planarity of the carboxylic and amide functional groups is predicted.
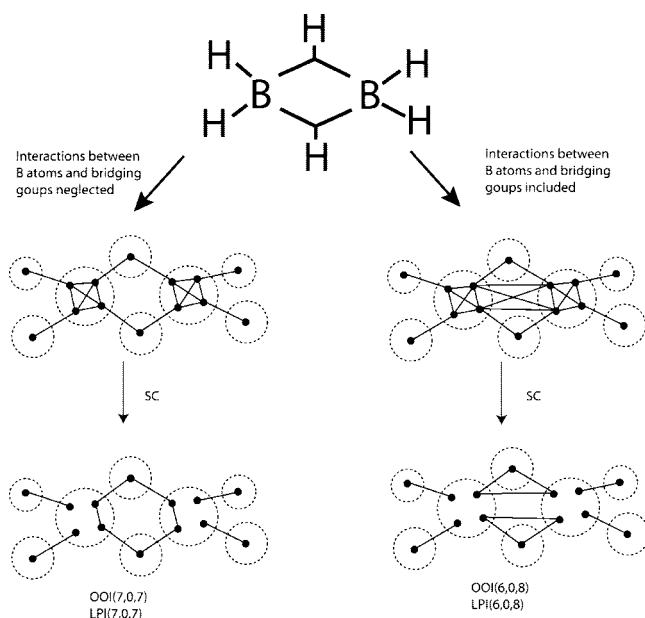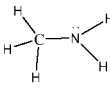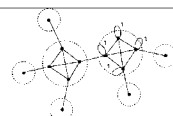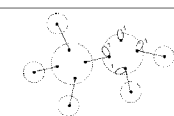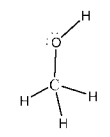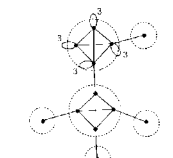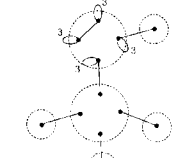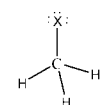

Figure 11. (Top) τ-Bonding representation of bridging BHB bonds in diborane. (Bottom) VIF pictures drawn according to the three-dimensional structure of diborane. VIF pictures on the *left* do not include interactions between the boron atoms and hydrogen bridges, while those on the *right* do. Application of the VIF rules gives proper 3c/2e⁻ bonds when these interactions are included.

VIF pictures as one-electron density operators for methyl amine, methanol, and a generic methyl halide are shown in Table 3. The reduced VIF pictures bear close resemblance to the bond-pair−lone pair arrangements expected in these molecules. The orbital occupancy indices, OOI, also give the numbers of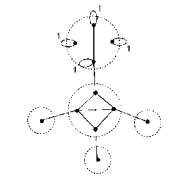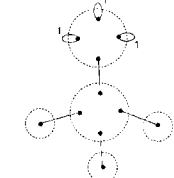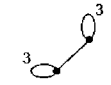 doubly, singly, and unoccupied valence orbitals expected. Results for R groups larger than methyl would be analogous. The nitrogen atom in methyl amine and the oxygen atom in methanol are given sp^3 hybridization according to their known molecular

TABLE 3: Lewis Structures, VIF Pictures, Reduced VIF Pictures, and OOI for Methyl Amine, Methanol, Methyl Halide and Some Resulting VIF Fragments[a]

species	VIF	Reduced VIF	OOI
			7, 0, 6
			7, 0, 5
			7, 0, 4
Oxygen lone pair fragment in methanol			**2, 0, 0**

[a] Correct numbers of doubly, singly, and unoccupied valence orbitals are predicted and recorded in the OOI. Reduced VIF pictures indicate bond connectivity and lone pair electron positions consistent with Lewis structures for these molecules and B3LYP6-311++Gdp NBO calculations.

geometries. For nitrogen in methyl amine, $\alpha_{Nsp3} = [2 + 3(3/3)]/(3 + 1) = 5/4$, $\beta_{Nsp3} = [2 - (3/3)]/(3 + 1) = 1/4$, and $\xi_{Nsp3} = [(5/4) - 1]/(1/4) = 1$. For oxygen in methanol, $\alpha_{Osp3} = 1/4(2 + 3(4/3)) = 3/2$, $\beta_{Osp3} = 1/4 (2 - (4/3)) = 1/6$, and $\xi_{Osp3} = (3/2 - 1)/(1/6) = 3$. In the methyl halide example, we expect two of the three halogen atom lone pairs to reside in orbitals that closely resemble p-orbitals centered on the halogen atom and therefore chose sp hybridization such that $\alpha_{Xsp} = [2 + 1(1/1)]/(1 + 1) = 3/2$, $\beta_{Xsp} = [2 - (1/1)]/(1 + 1) = 1/2$, and $\xi_{Xsp} = [(3/2) - 1]/(1/2) = 1$. Each example gives the correct number of valence electrons reflected in the OOI, expected bond pair−lone pair bonding scheme, and corresponds to hybridizations consistent with the molecule's known chemical and physical properties.

VIF pictures as one-electron Hamiltonian operators with a reference energy of $\alpha = -1/2 \, E_h$ are frequently the same as those for one-electron density operators with a reference orbital occupancy of one electron. One might therefore expect that the numbers of bonding, nonbonding, and antibonding orbitals with respect to $\alpha = -1/2 \, E_h$ expressed in the level pattern index, LPI to match the numbers of doubly, singly, and unoccupied orbitals enumerated in the orbital occupancy index, OOI. This possibility is investigated in the next section.

VIF Energy Pictures, NBO Energies, and VSEPR. Table 4 shows valence natural bond orbital, NBO, energies for methyl amine, methanol, methyl fluoride, methyl chloride, and methyl bromide calculated using B3LYP 6-311++Gdp. The same VIF pictures shown in Table 2 and Table 3 as one-electron density

TABLE 4: Valence NBO Energies Calculated for Methyl Amine, Methanol, Methyl Fluoride, Methyl Chloride, and Methyl Bromide[a]

Bond Pairs			Lone Pairs	
methyl amine	Methanol	methyl fluoride	methyl chloride	methyl bromide
0.435				
0.435	0.430			
0.400	0.389	0.364	0.377	0.385
0.400	0.376	0.364	0.377	0.385
0.389	0.376	0.364	0.377	0.385
0.353	0.279	0.208	0.099	0.050
-0.305	-0.302	-0.397	-0.314	-0.292
-0.502	-0.517	-0.397	-0.314	-0.292
-0.502	-0.521	-0.544	-0.552	-0.554
-0.505	-0.521	-0.544	-0.552	-0.554
-0.612	-0.614	-0.544	-0.552	-0.554
-0.612	-0.717	-0.919	-0.658	-0.595
-0.719	-0.818	-1.043	-0.902	-0.933
OOI(7,0, 6)	OOI(7, 0, 5)	OOI(7, 0, 4)	OOI(7, 0, 4)	OOI(7, 0, 4)
LPI(7,0, 6)	LPI(7, 0, 5)	LPI(7, 0, 4)	LPI(7, 0, 4)	LPI(7, 0, 4)

[a] Bond orbital energies are highlighted with blue, and lone pair orbital energies with red. OOI and LPI from VIF pictures are at the bottom of each column. Discrepancy of VIF LPI with computed energies can be understood by applying VSEPR theory.

operators can be interpreted as one-electron Hamiltonian operators with numbers of positive, zero, and negative eigenvalues with respect to $-1/2\ E_h$ enumerated in the level pattern index, LPI(n_+, n_0, n_-) numerically the same as their OOI. All of the OOI from Table 2 and Table 3 match the orbital occupancies for the molecules. Bond pair orbital energies are highlighted in blue and lone pair energies in red in Table 4. We see that there are discrepancies between the calculated energies and the LPI derived from VIF pictures. For methyl amine for example, there are six orbitals lower in energy than $-1/2\ E_h$ rather than seven predicted by the LPI.

Closer examination of the values in Table 4 reveals that all of the calculated energies that are in disagreement with LPIs derived from VIF pictures are energies for lone pair orbitals. One may hypothesize that the discrepancy is due to the percent s and percent p character in the lone pair hybrid orbitals. This explanation is not valid. The sp³ orbital for nitrogen calculated with valence orbital ionization energies, VOIE, has an energy of -15.8 eV $= -0.581\ E_h$. Likewise valence p-orbitals for oxygen, fluorine, and chlorine have respective VOIEs of -14.8 eV $= -0.544\ E_h$, -18.1 eV $= -0.665\ E_h$, and -15.0 eV $= -0.555\ E_h$. A better explanation for the discrepancy between calculated NBO energies and LPIs derived from VIF pictures is the effect of Coulombic and exchange energies that are included in the DFT B3LYP method but not in the VIF method. One can therefore easily understand these instances in which lone pair orbitals are higher in energy than predicted using VIF pictures as one-electron Hamiltonian operators by applying the VSEPR theory. Lone pair p-type NBOs are more subject to

VSEPR effects than σ-type lone pairs which are frequently the lowest energy NBO valence orbitals.

VI. Summary and Conclusions

Structurally covariant valency interaction formulas are given three chemical interpretations and applied to a variety of key chemical bonding motifs, two-center bonds with one, two, and three electrons, three-center bonds with two, three, and four electrons, ring systems with $4n+2$ and $4n$ electrons, diborane, and also to molecules with common functional groups, carboxylic acids, amides, ammines, alcohols, and halides. For the simplest case, of the hydrogen molecule, it is shown how the VIF rules are linear transformations and how sets of VIF pictures related by these rules correspond to numbers of doubly, singly, and unoccupied orbitals, or numbers of bonding, nonbonding, and antibonding orbitals, resonance structures, and LCAO wave functions (*interpretation 1*). These results for H_2 can be applied in a wide range of molecular species. It was found that VIF pictures as one-electron density operators that conform to the known numbers of doubly, singly, and unoccupied orbitals predict symmetries of $4n$ and $4n+2$ π-electron conjugated ring systems, the experimentally observed π-distortivity of benzene, regions of high spin density in allyl and benzyl radicals, τ-bonds in diborane, and correct planar geometries of carboxylic acid and amide functional groups. Predictions consistent with the conrotatory and disrotatory ring closures of allyl anion and cation, respectively, are made (*interpretation 2*). Conclusions drawn using VIF pictures and the VIF rules are supported by optimized molecular geometries using B3LYP6-311++Gdp and comparison with density elements computed by Wienhold and using HF STO-3G. VIF description of chemical bonding motifs including 2c/1e⁻, 2c/2e⁻, 2c/3e⁻, 3c/2e⁻, and 3c/4e⁻ bonds, lone pairs, radical electrons, and delocalized electrons agree well with computational MO and NBO methods.

The same VIF pictures drawn as one-electron density operators with a reference density of one electron per orbital can be interpreted as one-electron Hamiltonian operators with a reference of $-1/2\ E_h$ (*interpretation 3*). This allows the VIF results to be compared with valence NBO energies computed using B3LYP6-311++Gdp and discrepancies to be understood in terms of VSEPR theory.

VII. Future Work

A major goal of this work has been to demonstrate how quantum mechanically derived molecular structural formulas, VIF pictures, as related by the theory of structural covariance are applied to a variety of important chemical bonding motifs, 2c/1e⁻, 2c/2e⁻, 2c/3e⁻, 3c/2e⁻, 3c/3e⁻, 3c/4e⁻, $4n$ antiaromatic, and $4n+2$ aromatic, and bond pairs and lone pairs in some common functional groups. Future work will be to extend these ideas toward understanding a wider range of chemical bonding types and concerted chemical reactions.

References and Notes

(1) Pauling, L. C. *"Modern Structural Chemistry'*, Nobel Lecture, December 11 1954.

Valency Interaction Formulas to Predict Molecular Properties

J. Phys. Chem. A, Vol. 112, No. 40, 2008 **9795**

(2) Ingold, C. K. "Principles of an Electronic Theory of Organic Reactions". *(1934)Chemical Reviews* **1934**, *15*, 225–274.

(3) Jahn, H. A.; Teller, E. "Stability of Polyatomic Molecules in Degenerate Electronic States. I. Orbital Degeneracy. *Proc. R. Soc. London A* **1937**, *161*, 220.

(4) Hückel, E. "Quantum-theoretical contributions to the benzene problem. I. The electron configuration of benzene and related compounds". *Z. Physik* **1931**, *71*, 204–286.

(5) (a) Breslow, R. *Chem. Eng. News* **1965**, 90–99. (b) Breslow, R. *Acc. Chem. Res.* **1973**, *6*, 393–398.

(6) Shaik, S. S.; Hiberty, P. C. *A Chemist's Guide to Valence Bond Theory, Wiley-Interscience* **2008**, page 13.

(7) Wheland, G. H. Pauling, Linus, "A Quantum Mechanical Discussion of Orientation of Substituents in Aromatic Molecules". *J. Am. Chem. Soc.* **1935 57**, (11), 2086–2095.

(8) Sinanoglu, O. *Chem. Phys. Lett.* **1984**, *103* (4), 315–322.

(9) Sinanoglu, O.; Alia, J.; Hastings, M. *J. Phys. Chem.* **1994**, *98*, 5867–5877.

(10) Alia, J. *"Molecular Structural Formulas as One-Elelctron Density and Hamiltonian Operators: The VIF Method Extended" J. Phys. Chem. A* **2007**, *111* (12), 2307–2318.

(11) Weinhold, F.; Landis, C. *Valency and Bonding: A Natural Bond Orbital Donor-Acceptor Perspective. Cambridge University Press, Cambridge* **2005**,

(12) Gillespie, R.; Hargittai, I. *The VSEPR Model of Molecular Geometry, Allyn and Bacon, Boston* **1991**,

(13) (a) Sinanoglu, O. "On the algebraic construction of chemistry from quantum mechanics. A fundamental valency vector field defined on the Euclidean 3-space and its relation to Hilbert space". *Theoret. Chim. Acta (Berl.)* **1984**, *65*, 243–248. (b) Sinanoglu, O. "A principle of linear covariance for quantum mechanics and electronic structure theory of molecules and other atom clusters". *Theoret. Chim. Acta (Berl.)* **1984**, *6*, 233–242. (c) Sinanoglu, O. Non-unitary classification of molecular electronic structures and other atom clusters". *Theoret. Chim. Acta (Berl.)* **1984**, *6*, 249–254. (d) Sinanoglu, O. "Structural Covariance of Graphs".

Theoret. Chim. Acta (Berl.) **1984**, *6*, 255–265. (e) Sinanoglu, O. "Deformational Covariance of Graphs". *Theoret. Chim. Acta (Berl.)* **1984**, *6*, 267–270.

(14) Pauling, L. *J. Am. Chem. Soc.* **1931**, *53*, 1367.

(15) Frisch, M. J.; Trucks, G. W.; Schlegel, H. B.; Scuseria, G. E.; Robb, M. A.; Cheeseman, J. R.; Montgomery, J. A., Jr.; Vreven, T., Kudin, K. N.; Burant, J. C.; Millam, J. M., Iyengar, S. S.; Tomasi, J.; Barone, V.; Mennucci, B.; Cossi, M.; Scalmani, G.; Rega, N.; Petersson, G. A.; Nakatsuji, H.; Hada, M.; Ehara, M.; Toyota, K.; Fukuda, R.; Hasegawa, J.; Ishida, M.; Nakajima, T.; Honda, Y.; Kitao, O.; Nakai, H. , Klene, M.; Li, X.; Knox, J. E.; Hratchian, H. P., Cross, J. B.; Adamo, C.; Jaramillo, J.; Gomperts, R.; Stratmann, R. E.; Yazyev, O.; Austin, A. J.; Cammi, R.; Pomelli, C.; Ochterski, J. W.; Ayala, P. Y.; Morokuma, K.; Voth, G. A.; Salvador, P.; Dannenberg, J. J.; Zakrzewski, V. G.; Dapprich, S.; Daniels, A. D.; Strain, M. C.; Farkas, O. ; Malick, D. K.; Rabuck, A. D.; Raghavachari, K.; Foresman; J. B.; Ortiz, J. V.; Cui, Q.; Baboul, A. G.; Clifford, S.; Cioslowski, J.; Stefanov, B. B.; Liu, G.; Liashenko, A.; Piskorz, P.; Komaromi, I.; Martin, R. L.; Fox, D. J.; Keith, T.; Al-Laham, M. A.; Peng, C. Y.; Nanayakkara, A.; Challacombe, M.; Gill, P. M. W.; Johnson, B.; Chen, W.; Wong, M. W.; Gonzalez, C.; Pople, J. A. *Gaussian 03*, Revision C.02; Gaussian, Inc.: Wallingford, CT, 2004.

(16) (a) Woodward, R. B.; Hoffman, R. *The Conservation of Orbital Symmetry*; Verlag Chemie GmbH Academic Press, Inc.: Berlin, 1970; p 45. (b) Boche, G.; Martens, D. *Angew. Chem., Int. Ed. Engl.* **1972**, *11* (8), 724–725. (c) Faza, O. N.; Lopez, C. S.; Alvarez, R.; de Lera, A. R. *Org. Lett.* **2004**, *6* (6), 901–904.

(17) (a) Berry, R. S. *J. Chem. Phys.* **1961**, *35*, 2253. (b) Shaik, S.; Shurki, A.; Danovich, D.; Hiberty, P. C. *Chem. Rev.* **2001**, *101*, 1501–1539.

(18) Price, W. C. *J. Chem. Phys.* **1947**, *15*, 614.

(19) (a) Lipscomb, W. N. *Boron Hydrides*; W. A. Benjamin: New York, 1963. (b) http://nobelprize.org/nobel_prizes/chemistry/laureates/, 1976.